

# Geochemistry of mafic dykes in part of Chotanagpur gneissic complex: Petrogenetic and tectonic implications

AKASH KUMAR and TALAT AHMAD\*

Department of Geology, University of Delhi, Delhi-110007, India

(Received June 1, 2006; Accepted February 21, 2007)

Chotanagpur Gneissic Complex basement rocks of the Eastern Indian shield has been dissected by numerous mafic dykes, now occurring as amphibolitic dykes and gneissic amphibolites. These dykes are subalkaline, ranging in composition from basalt through basaltic-andesite to andesite. These rocks have enriched incompatible trace element patterns. These are particularly enriched in light rare earth elements (LREE) and large ion lithophile elements (LILE) with depleted high field strength elements (HFSE; Nb, P, Ti) characteristics (i). Negative Sr anomaly is conspicuous. Nb/La and Nb/Ce ratios of the dykes are lower compared to the primitive mantle but these values are closer to average crustal values. Incompatible trace element data suggest enriched source characteristics and influence of crustal contamination in their genesis. Trace element ratios such as Gd/Yb of these dykes indicate at least two different sources. They probably represent Precambrian continental rifting in this region.

Keywords: Chotanagpur gneissic complex, amphibolitic dykes, continental rifting, trace elements

## INTRODUCTION

The Chotanagpur Gneissic Complex (CGC) province of the eastern Indian shield has been traversed by numerous mafic dykes for which little information is available (Ghosh *et al.*, 2005). These dykes occur in the form of amphibolitic dykes, gneissic amphibolites and some doleritic dykes. Most of these dykes are Precambrian as they do not traverse through the overlying Permian Gondwana sequence (Mahadevan, 2002). We have studied the Precambrian mafic dykes to understand their nature, geochemical characteristics and their genesis. The latter will help us understand the evolution and nature of the Precambrian sub-continental mantle sources and the processes that these sources regions must have suffered before or during the generation of these dykes. It will also help us understand the Precambrian plate tectonic scenario that was active in this region.

## GEOLOGICAL SETTING OF THE STUDY AREA

Mafic dykes of the Indian shield have been studied since mid-nineteenth century (Clarke, 1869) and their occurrence as swarms and networks of regional persistence has been detailed (Pascoe, 1950). The evolution of the Indian Shield was marked by four major episodes of basic magmatism based on litho-stratigraphic association

(Divakara Rao *et al.*, 1984). These associations are: (1) Archean mafic and ultramafic sequences occurring in the Dharwar, Singhbhum and Aravalli cratons and xenoliths observed in the associated granitic gneisses; (2) calc-alkaline and tholeiitic basalts in Proterozoic basins; (3) Cenozoic to Paleozoic volcanic rocks associated with different phases of the Himalayan orogeny; and (4) Cenozoic-Mesozoic tholeiitic flood basalts (Deccan and Rajmahal Traps). Here a part of Singhbhum-Chotanagpur craton is under investigation. The eastern Indian shield consists of two major crustal provinces *viz.*, Singhbhum crustal province and Chotanagpur gneissic province (CGC) (Ghosh *et al.*, 2005). The Singhbhum Proterozoic basin has a tectonic boundary with the northern high-grade metamorphic migmatite belt of the CGC, trending parallel to the basinal axis (Bose, 1990). It contains more than ninety percent of Archean rocks dominated by granites, gneisses and migmatites. The pre-tectonic igneous activity is characterized by small bodies of ultramafic intrusion (Bose, 1990). The country rocks were folded and metamorphosed during the Satpura orogeny ( $900 \pm 200$  Ma) (Sarkar, 1968; Ghosh *et al.*, 1973; Gupta, 1973). The rocks of the CGC have undergone predominantly amphibolite facies metamorphism (Mahadevan, 2002). Bhattacharya (1976) described an increase in the grade of metamorphism from the western part to the eastern, where typical granulite facies rocks are present. It has also been shown that the metamorphic grade decreases from north towards south in the CGC (Banerji, 1991). However, this seems to be only a broad generalization

\*Corresponding author (e-mail: tahmad001@yahoo.co.in)

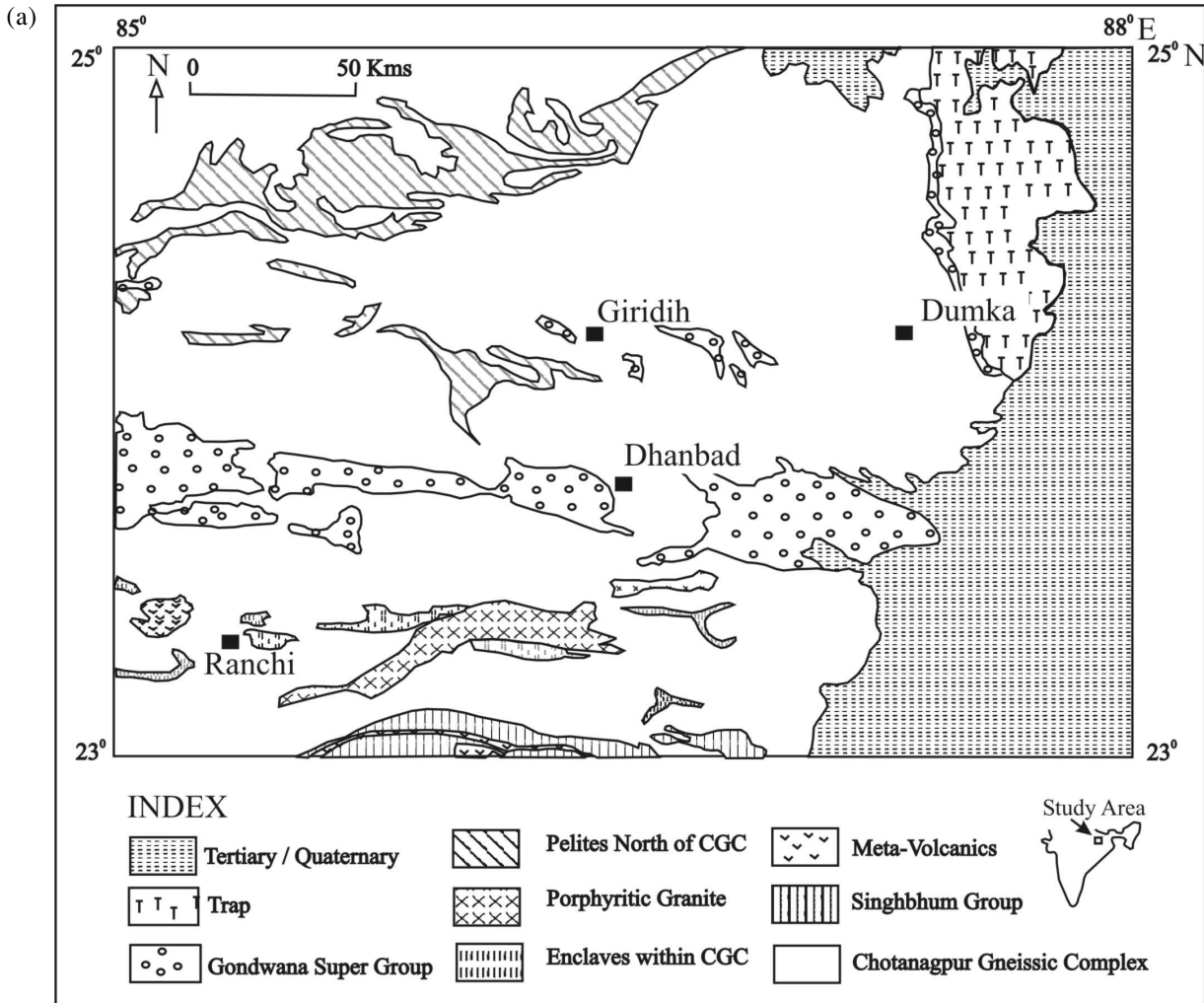


Fig. 1. (a) Generalized geological map of Chotanagpur Cratonic part (Modified after Mazumdar, 1988). (b) Geological map of Chotanagpur and Singhbhum regions showing major mafic dyke swarms (Modified after Murthy, 1987).

because a comprehensive view of metamorphic episode has not emerged due to the lack of geochronological data and systematic regional evaluation. Geologically, the CGC is an extension of the Satpura regions including Sausar Group of Central India based on the continuation of ENE-WSW strike of the formation (Holmes, 1955; Saha, 1994; Mahadevan, 2002; Acharyya, 2001). Based on the lithological similarities and spatial disposition, Singh (1998) proposed a correlation of the formations of the CGC with those from Singhbhum on one hand and with the formation of Central India and Rajasthan on the other. The area has undergone three phases of deformation producing distinctive folds (F1, F2 and F3) and related linear fabric (Sengupta and Sarkar, 1964; Ghosh, 1971, 1983; Chattopadhyay and Saha, 1974; Bhattacharya, 1975; Sarkar, 1977, 1988; Chatterjee and Sengupta, 1980). The structural evolution of the region is marked by a first gen-

eration of isoclinal folding, followed by a second phase of fold movement that gave rise to antiformal and synformal structures on the foliation from the surface (Bhattacharya, 1975). The axial trend in the central and northern part of the area is dominantly N-S but veers to the SW in the south western part. This phase (second) of folding is marked by the intrusion of several syntectonic small bodies of basic igneous rocks that have shared the high-grade metamorphism along with the host rocks (Bhattacharya, 1975). Finally, probably last and third phase of folding with NW-trending axial trace has affected the earlier folds giving rise to several macroscopic structural domes and basins. The metasediments and the gneissic rocks have been profusely intruded by basic rocks now represented by amphibolite, metadolerite, metanorite, metagabbro and pyroxene granulites (Figs. 1b, 2a and 2b). These mafic-ultramafic intrusives preceded the major

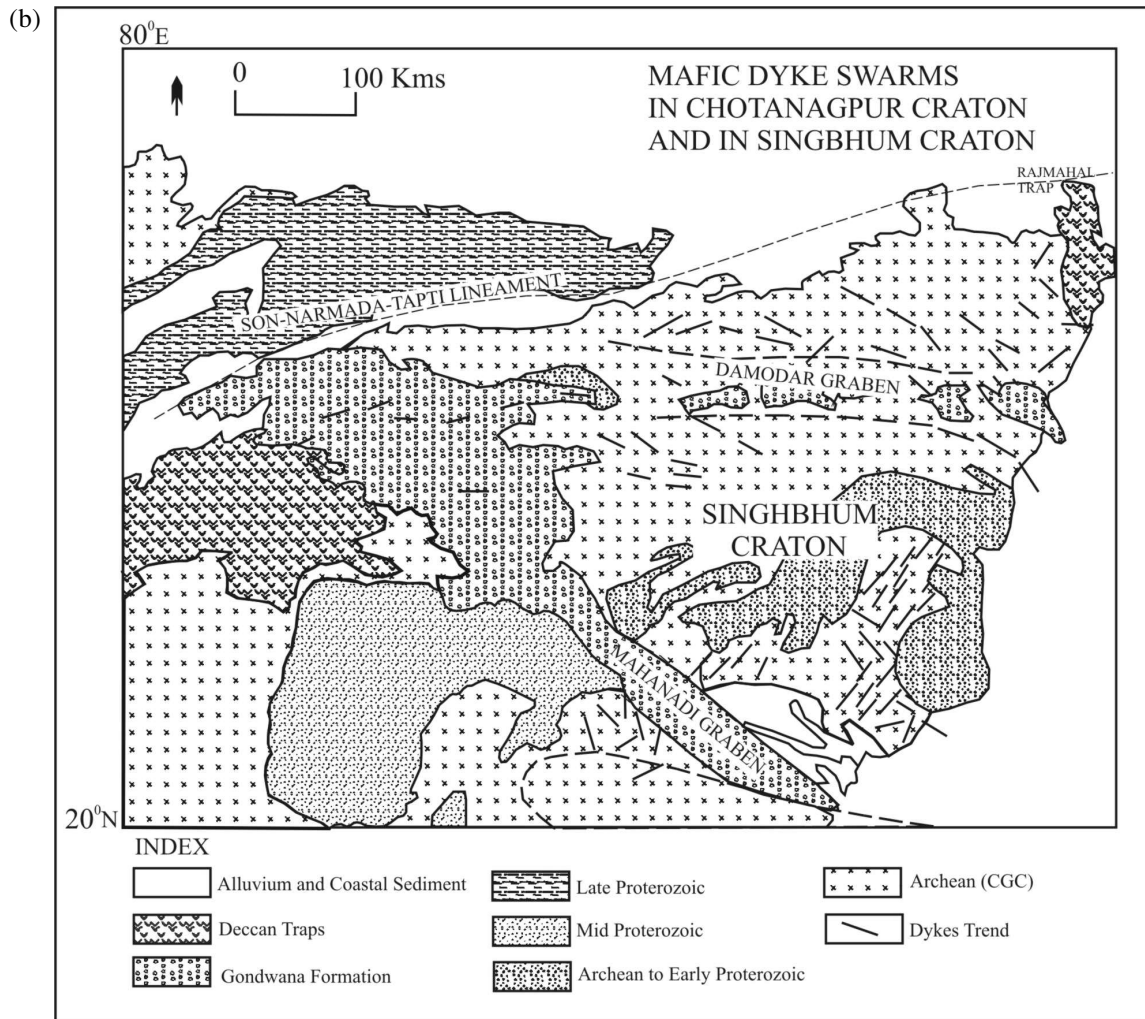


Fig. 1. (continued).

granitic activity at 1600 Ma (Pandey *et al.*, 1986) as evident from the occurrence of the former as enclaves within latter. The general trends of these mafic bodies are NW-SE. These metaigneous rocks are generally concordant with the foliation of the host rocks, though local discordance is not uncommon. Large numbers of these bodies are a few centimeters in thickness and meters to decameters in dimension (Figs. 2a and 2b), thus they are far below mapable dimensions and, therefore, remain under-represented in most geological map (Mahadevan, 2002). Predominant among these are the amphibolites, the major rock type under consideration in this study. Gondwana fluvial deposits border the western part of the Chotanagpur terrain. Depositions of Gondwana metasediments in Damodar valley occur in patches dividing the CGC into northern and southern parts (Fig. 1a). Kimberlite intrusives occur in the southwest of the Rajmahal trap. Sr-Nd-Pb isotopic studies of kimberlite

from Rajmahal province suggest influence of Kerguelen plume in the generation of these magmas. The Kerguelen hotspot was responsible for the ~117 Ma magmatic activity in Eastern Indian Shield (Kumar *et al.*, 2003). Lamprophyric sills are also reported from Jharia basin, their Sr, Nd and Pb ratios are similar to isotopic ratios of kimberlite from Rajmahal trap (Rock *et al.*, 1992).

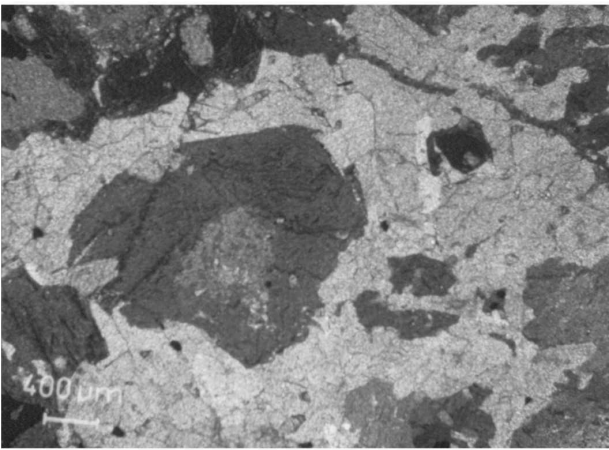
The amphibolitic dykes mainly occur as discontinuous patches and boulders in the study area (Figs. 2a and 2b). Exposures of granitoid at Dhahiya village (N23°48'2.0" and E86°26'55") contain the rapakivi structure. The structure is typically developed in post-orogenic granites emplaced at shallow level within crust (Bose, 1997). Structural complexities between amphibolitic dykes and gneisses are present at Khudia Nala near Govindpur, on Govindpur-Giridih road (Fig. 1a). Here some amphibolitic bodies present are not folded with gneisses but others are co-folded with basement gneisses,



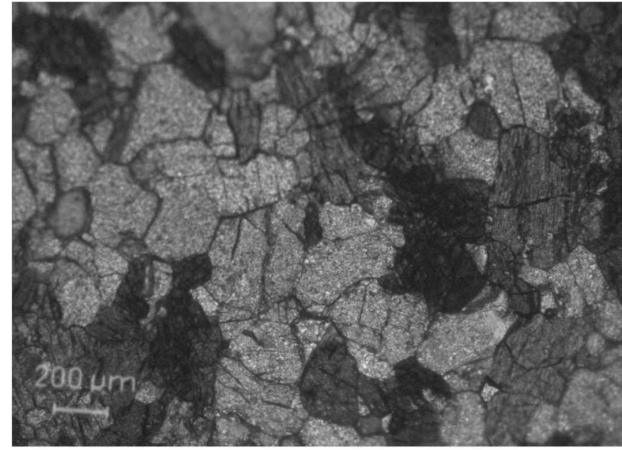
(a)



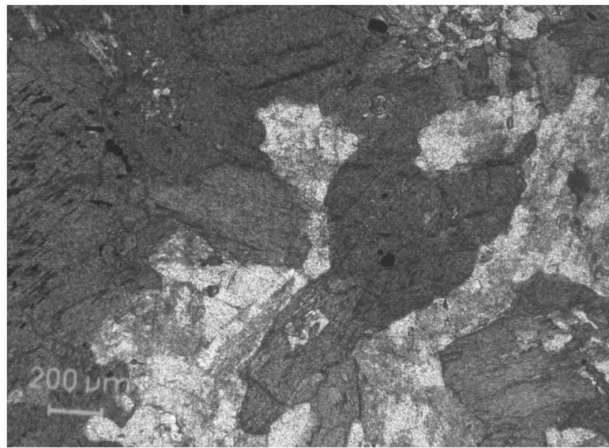
(b)



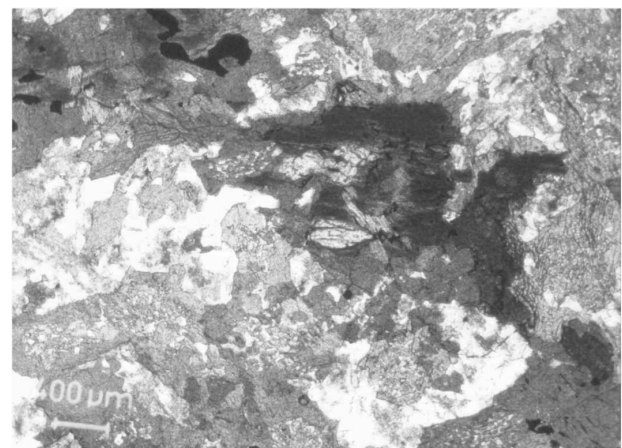
(c)



(d)



(e)



(f)

*Fig. 2. (a) and (b) Field photographs showing occurrence of the amphibolitic dykes traversing through the Chotanagpur Gneissic Complex in Khudia Nala section on Tundi-Giridih road. (c) Relict grains of clinopyroxene rimmed by amphiboles are shown along with Ophitic textures. (d) Equigranular, less altered and mildly deformed variety of amphibolitic dyke (Group 3). (e) Alteration of amphibole to Biotite and Plagioclase saussuritization are present. (f) Clinopyroxene alteration into amphiboles and in turn amphiboles to biotite are seen in a row.*

probably indicating more than one generation of mafic dykes in this region.

### *Petrography*

The amphibolites of the study area are dark green to black at times very hard and massive, medium to coarse grained. They are often foliated with fabrics defined by alignment of amphiboles and banded with amphibole and feldspar rich layers. The rocks contain pyroxenes, amphibole (hornblende), feldspars (plagioclase and K-feldspars), biotite, magnetite and Quartz. Feldspars occur both as phenocrysts and groundmass. The presence of feldspar in the rock samples are well matched with positive Eu- and Sr-anomalies in the multi-element patterns. Augite is the dominant pyroxene, which occurs as euhedral to subhedral phenocrysts and also as fine grained groundmass. Some of the amphibole (hbl) may have formed due to the alteration of augite at late magmatic stage as suggested by parallelism of hornblende with augite and at some places the former makes a reaction rim around augite crystals. Ophitic to sub-ophitic relationships between plagioclase and clinopyroxene phenocrysts is common (Fig. 2c). On the basis of petrography we can sub-divide our samples in three groups (amphibolite Group 1, 2 and 3). Samples of amphibolite Group 1 and 2 are medium to coarse grain, partly altered and inequigranular. In these rocks plagioclase feldspar is more abundant. In comparison to amphibolite (Group 1 and 2), amphibolite (Group 3) samples are fine to medium grained, equigranular, relatively fresh and less deformed (Fig. 2d). These two groups occur in two different locations in the study area.

Post crystallization deformation can be visualized by the presence of highly fractured phenocrysts of feldspars and deformation lamellae in plagioclase. Rounded corners of feldspar phenocrysts indicate event of magmatic corrosion. Plagioclase crystals are often saussuritised (Fig. 2e). Biotite retrograde reaction rim is present around amphiboles (Fig. 2f). Some amphiboles grains are zoned, it may either be due to deformation or compositional variations.

Gneissic amphibolites are characterized by the presence of gneissose structure. Laths of amphibole (hbl), pyroxenes and biotite display strong preferred orientations. Bands of quartz and feldspar grains are also present, but the bands are not continuous. In these rocks igneous texture is obliterated to a large extent.

## **GEOCHEMISTRY**

### *Analytical techniques*

Representative amphibolitic dykes and gneissic amphibolites samples, collected from wide separated localities from the study area (Figs. 1a and 1b) were bro-

ken into small pieces using steel mortar. These were then reduced into small chips using jaw-crusher. These were thoroughly homogenized before they were made into fine powder of -230 mesh using ball mills. The fine powdered samples were used for the analyses of major and trace elements (including the rare earth elements). Major and trace elements analysis were carried out at Wadia Institute of Himalayan Geology, Dehradun using WD-XRF (Siemens SRS 3000) following the procedure of (Saini *et al.*, 1998). The rare earth elements were determined at Wadia Institute using ICP-MS (Perkin Elmer, ELAN DRC-e). Precision and accuracy for ICP-MS technique is given in Ahmad *et al.* (2005) and Rao and Rai (2006). The analytical data are presented in Table 1. The table also shows analyzed and reported values for the rock standards (Rao and Rai, 2006).

### *Elemental mobility*

Alteration effects can be seen in the field and also through petrographic studies. Growth of secondary minerals like chlorite, epidote, biotite, sometimes amphiboles are used as parameters to understand the degree of alteration. Limited growth of these minerals at grain boundary may develop due to the interaction with late magmatic fluids and thus are considered isochemical (Pollard *et al.*, 1983; Taylor and Pollard, 1988).

In addition to petrographic study the alteration effects can also be evaluated through geochemical variation diagram known as Harker diagram (Figs. 3.1 and 3.2). The rocks under consideration have undergone some alteration as seen from the petrographic description. The distribution of some of the elements must have been disturbed due to the secondary processes.

Figure 3.1 is a series of binary plots where all the major elements are plotted against Zr. During low-grade metamorphism Zr is considered to be relatively immobile (Floyd and Lees, 1973; Winchester and Floyd, 1977; Macdonald *et al.*, 1988). Hence, Zr can be used as a parameter for evaluating the elemental mobility and also to understand the differentiation of magma. Most of the major elements including Fe<sub>2</sub>O<sub>3</sub>, MgO, CaO and Al<sub>2</sub>O<sub>3</sub> show negative relationship with Zr. P<sub>2</sub>O<sub>5</sub> and to some extent TiO<sub>2</sub> show an initial increase in the basaltic composition and then a negative trend in the intermediate to acidic end, probably indicating titanite and apatite fractionation (Ahmad and Tarney, 1991). These negative relationships probably indicate near primary magmatic characteristics for these major elements. In Zr-Al<sub>2</sub>O<sub>3</sub> plot amphibolitic dyke form two broad sub-groups on the basis of Al<sub>2</sub>O<sub>3</sub> content. Their negative relationships indicate their primary magmatic characteristics but horizontal shift may indicate slightly different sources or two separate events of magmatism from similar sources (Fig. 3.1A). In Zr-Na<sub>2</sub>O plot (Fig. 3.1F), the scattering of data

Table 1. Representative major (wt%) and trace (ppm) elemental abundances of Amphibolitic dykes and Gneissic Amphibolites from Dhanbad District, Jharkhand

Sample	Amphibolitic dykes (Group 1 and 2)										Amphibolitic dykes (Group 3)				
	1A	2C	3A	3D	4B	4F	5B	6C	Mean (n = 19)	S.D.	7A	7B	8	Mean (n = 3)	S.D.
SiO <sub>2</sub>	51.08	51.87	51.69	51.02	50.19	47.71	46.65	51.15	49.99	2.04	50.48	50.09	48.06	49.54	1.30
TiO <sub>2</sub>	1.98	1.20	1.42	1.57	1.04	0.99	1.38	1.70	1.47	0.37	0.68	0.64	0.98	0.77	0.19
Al <sub>2</sub> O <sub>3</sub>	12.04	13.70	14.03	11.90	12.80	14.10	12.34	14.29	13.36	0.85	13.34	12.39	12.24	12.66	0.60
Fe <sub>2</sub> O <sub>3</sub>	13.98	10.97	10.85	13.56	13.22	12.94	15.58	11.65	12.76	1.67	10.68	10.42	13.01	11.37	1.43
MnO	0.22	0.18	0.17	0.17	0.20	0.17	0.24	0.17	0.19	0.03	0.23	0.22	0.22	0.22	0.01
MgO	5.96	7.55	7.34	8.01	7.62	7.77	6.69	6.41	7.02	0.70	7.13	8.81	7.47	7.80	0.89
CaO	8.84	7.81	9.50	7.69	9.54	9.80	10.19	9.29	9.17	0.82	10.60	10.71	11.68	11.00	0.59
Na <sub>2</sub> O	2.13	2.06	1.92	1.73	1.86	1.99	2.48	2.27	2.07	0.20	3.71	3.16	2.67	3.18	0.52
K <sub>2</sub> O	1.58	1.94	1.26	1.46	0.74	0.90	1.88	1.51	1.45	0.48	0.68	0.54	0.84	0.69	0.15
P <sub>2</sub> O <sub>5</sub>	0.29	0.47	0.29	0.31	0.23	0.23	0.16	0.37	0.36	0.26	0.31	0.29	0.20	0.27	0.06
LOI	0.43	0.76	0.25	2.65	0.88	2.64	0.60	0.37	0.75	0.75	0.43	0.57	0.37	0.45	0.10
Total	98.53	98.51	98.72	100.07	98.32	99.24	98.19	99.18	98.58	0.74	98.27	97.84	97.74	97.95	0.28
Rb	74	59	46	65	21	24	68	52	51.60	19.80	8	7	11	8.67	2.08
Sr	148	347	167	104	304	382	169	186	227.20	96.14	334	250	161	248.30	86.51
Y	42	34	46	50	31	35	40	44	40.21	8.66	19	25	6	16.70	10.12
Zr	170	227	164	207	116	110	85	176	162.40	53.49	111	146	60	105.70	43.25
Nb	13	9	12	10	4	4	4	12	9.50	4.48	6	7	4	5.77	1.56
Ba	259	628	239	219	208	239	100	285	299.78	181.49	89	39	22	50.00	34.80
Sc	28	22	25	34	28	31	42	26	29.07	5.73	20	29	19	22.56	5.49
V	127	36	42	225	203	263	67	194	144.92	78.93	85	84	140	102.95	32.00
Cr	319	432	342	493	217	313	198	286	298.88	104.13	83	312	102	165.70	127.10
Co	43	40	43	45	44	50	49	45	44.40	2.79	41	44	49	44.70	4.04
Ni	110	193	132	154	121	176	118	162	139.10	27.69	77	133	81	97.00	31.24
Cu	27	48	28	36	22	51	118	37	44.26	27.47	7	8	8	7.70	0.58
Zn	146	102	95	106	113	107	135	105	113.10	16.24	110	121	152	127.70	21.78
Ga	19	16	17	19	17	20	18	21	18.22	1.43	15	15	15	15.10	0.52
La	21.70	41.85	24.00	29.25	26.84	24.34	11.70	35.00	26.73	9.49	19.70	24.78	9.33	17.94	7.87
Ce	51.36	91.20	54.43	66.01	56.84	52.80	21.90	83.30	59.70	20.63	47.10	53.02	19.06	39.73	18.14
Pr	6.99	11.28	7.46	8.20	6.71	6.50	3.92	10.04	7.70	2.64	6.16	7.36	2.46	5.33	2.55
Nd	28.64	40.88	28.60	31.78	24.98	24.68	17.26	38.92	29.81	9.43	24.88	28.80	9.88	21.19	9.99
Sm	6.65	6.78	5.81	7.48	4.84	5.18	4.46	8.45	6.26	1.43	5.60	6.15	2.09	4.61	2.20
Eu	1.62	1.43	1.23	1.55	1.37	1.55	1.22	1.76	1.51	0.23	1.60	1.64	0.56	1.27	0.61
Gd	7.06	5.14	5.28	8.40	5.30	5.64	4.48	9.18	6.26	1.38	5.26	5.95	2.12	4.44	2.04
Tb	1.16	0.86	0.96	1.36	0.83	0.95	0.87	1.45	1.04	0.20	0.74	0.88	0.31	0.64	0.30
Dy	7.12	6.20	7.36	8.01	4.99	5.75	7.05	8.38	6.82	1.38	3.94	4.92	1.71	3.52	1.65
Ho	1.47	1.32	1.68	1.76	1.09	1.28	1.59	1.77	1.49	0.30	0.77	0.98	0.33	0.69	0.33
Er	4.30	3.76	4.75	4.71	3.05	3.53	4.43	4.70	4.11	0.88	2.00	2.59	0.81	1.80	0.91
Tm	0.61	0.57	0.71	0.74	0.47	0.55	0.67	0.70	0.62	0.13	0.29	0.39	0.11	0.26	0.14
Yb	4.07	3.76	4.72	4.76	3.10	3.76	4.32	4.58	4.10	0.83	1.88	2.59	0.70	1.72	0.95
Lu	0.60	0.48	0.62	0.73	0.50	0.58	0.56	0.69	0.59	0.10	0.26	0.38	0.09	0.24	0.15

Sample	Gneissic					Analysed values (reported values) of standards	
	1B	2B	2F	5C	Mean (n = 9)	S.D.	GSR-3
SiO <sub>2</sub>	62.04	51.67	51.91	48.53	52.57	4.84	45.18 (44.64)
TiO <sub>2</sub>	1.09	1.11	1.65	0.64	1.08	0.34	2.38 (2.36)
Al <sub>2</sub> O <sub>3</sub>	13.57	14.10	14.39	12.41	13.27	0.86	13.77 (13.83)
Fe <sub>2</sub> O <sub>3</sub>	7.00	10.83	10.44	12.12	10.70	2.16	13.33 (13.40)
MnO	0.10	0.15	0.15	0.19	0.17	0.05	0.17 (0.17)
MgO	3.23	6.23	5.23	9.35	6.55	2.18	7.46 (7.77)
CaO	3.96	7.50	7.07	10.63	7.71	2.30	8.65 (8.81)
Na <sub>2</sub> O	2.26	2.33	2.71	2.09	2.20	0.26	3.51 (3.38)
K <sub>2</sub> O	4.83	2.23	3.09	1.53	2.64	1.05	2.36 (2.32)
P <sub>2</sub> O <sub>5</sub>	0.32	0.53	1.01	0.06	0.37	0.32	0.86 (0.95)
LOI	0.37	1.00	1.89	1.09	0.95	0.45	
Total	98.77	97.68	99.54	98.64	98.21	1.20	
Rb	155	68	100	73	96.43	34.00	JB-1a 38 (41)
Sr	138	442	469	159	271.40	174.90	448 (443)
Y	30	47	42	29	44.12	18.30	23.8 (24)
Zr	346	183	314	57	205.00	122.10	141 (146)
Nb	13	12	18	4	11.10	5.94	26 (27)
Ba	1052	837	1660	84	647.23	572.22	472 (497)
Sc	8	21	16	37	26.25	14.22	29 (28)
V	51	43	48	47	64.12	51.04	
Cr	278	188	107	457	264.24	143.08	435 (415)
Co	29	38	35	51	39.00	9.11	
Ni	147	123	90	212	149.70	43.57	133 (140)
Cu	20	43	26	98	45.60	32.70	60 (56)
Zn	97	112	119	98	106.30	7.97	
Ga	19	19	19	14	17.27	2.24	19 (18)
La	20.38	47.55	79.84	9.34	33.79	24.05	36.17 (38.10)
Ce	44.80	107.60	176.00	18.20	76.18	55.06	63.60 (66.10)
Pr	5.87	14.26	22.11	2.64	9.92	6.79	7.09 (7.30)
Nd	22.61	52.46	78.40	10.20	36.69	23.99	26.06 (25.50)
Sm	5.43	8.91	11.62	2.40	6.99	3.51	5.26 (5.07)
Eu	1.50	1.65	2.29	0.62	1.39	0.61	1.62 (1.47)
Gd	5.52	6.81	8.33	2.50	5.98	2.65	5.29 (4.54)
Tb	0.89	1.12	1.10	0.51	1.01	0.41	0.72 (0.69)
Dy	5.28	8.05	7.80	4.20	7.24	3.09	3.99(4.19)
Ho	1.12	1.75	1.69	1.00	1.61	0.69	0.79(0.64)
Er	3.01	4.94	4.59	3.00	4.60	2.03	2.13 (2.18)
Tm	0.47	0.74	0.68	0.47	0.70	0.31	0.31 (0.31)
Yb	3.10	4.89	4.35	3.15	4.68	2.07	2.10 (2.10)
Lu	0.47	0.62	0.59	0.43	0.63	0.24	0.32 (0.32)

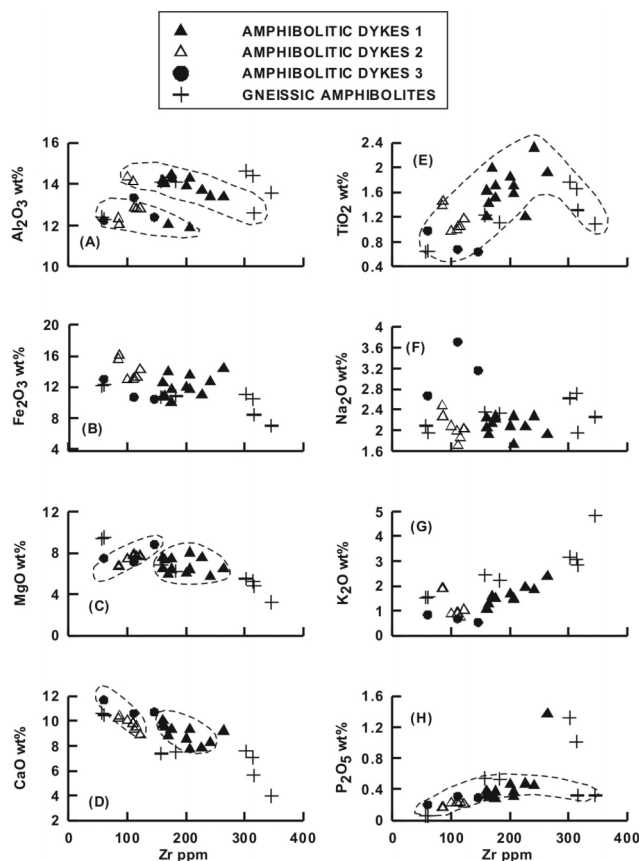


Fig. 3.1. Binary plots of (A) Zr vs.  $Al_2O_3$  (B) Zr vs.  $Fe_2O_3$  (C) Zr vs.  $MgO$  (D) Zr vs.  $CaO$  (E) Zr vs.  $TiO_2$  (F) Zr vs.  $Na_2O$  (G) Zr vs.  $K_2O$  and (H) Zr vs.  $P_2O_5$  for the amphibolitic dykes 1, 2, 3 and gneissic amphibolites from Jharkhand around Dhanbad.

points probably indicate the mobile nature of  $Na_2O$  during the post crystallization processes. Most of the other major elements including the  $K_2O$  show predictable magmatic trends when plotted against Zr (Fig. 3.1) and  $SiO_2$  (figures not shown here).

Figure 3.2 are series of binary plots where trace and rare earth elements Ni, Sc, Co, Rb, La, Nd and Nb are plotted against Zr and Nd plotted against La. These elements have different compatibilities for basaltic/gabbroic phases (olivine, orthopyroxene, clinopyroxene and plagioclase). These plots display magmatic trends with positive relationships between Nb–Zr, Rb–Zr, La–Zr, Nd–Zr, Nd–La and negative relationships between Co–Zr, Sc–Zr and to some extent Ni–Zr, the latter could have been affected by secondary processes to some extent. Thus, like most of the major elements, the trace elements also appear to have been least perturbed by post crystallisation processes and may represent near primary characteristics.

In Fig. 3.2E all the data plot towards La side compared to the primitive mantle ratio line for La/Nd and in

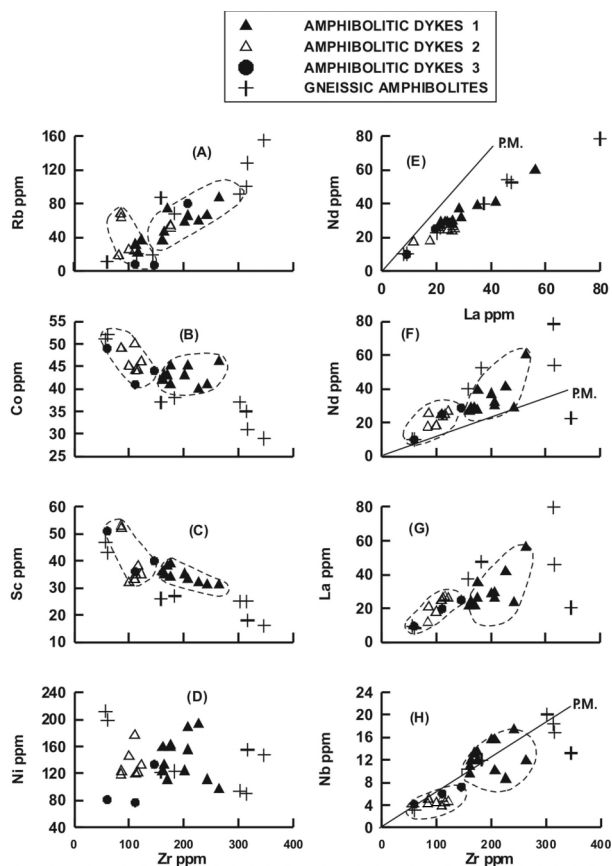


Fig. 3.2. Binary plots of (A) Zr vs. Rb (B) Zr vs. Co (C) Zr vs. Sc (D) Zr vs. Ni (E) La vs. Nd (F) Zr vs. Nb (G) Zr vs. La (H) Zr vs. Nb for the amphibolitic dykes 1, 2, 3 and gneissic amphibolites from Jharkhand around Dhanbad. Primitive mantle (P.M.) values after Sun and McDonough (1989).

Fig. 3.2F all the data plot towards Nd side with respect to primitive mantle for Zr/Nd. During melting of mantle sources La behaves more incompatibly than Nd and Nd is relatively more incompatible than Zr. Plots of the data points in these diagrams (Figs. 3.2E and F) indicate enriched nature of these samples and probably also their source(s) relative to primitive mantle. In Fig. 3.2H, although Nb is more incompatible than Zr, most of the data fall on the Zr side or close to primitive mantle ratio line indicating depletion of Nb with respect to Zr. The latter is a common feature observed in continental crust and sub-continental lithosphere, thus the plots in Fig. 3.2H probably indicate influence of these (continental crust and sub-continental lithosphere) in the genesis of these dykes.

Thus, the binary plots of major and trace elements (Figs. 3.1 and 3.2) indicate that all the major elements (except for  $Na_2O$ ), and the trace elements (except for Ni), have not been affected by post crystallisation secondary processes. At the same time data indicate their enriched trace element characteristics.

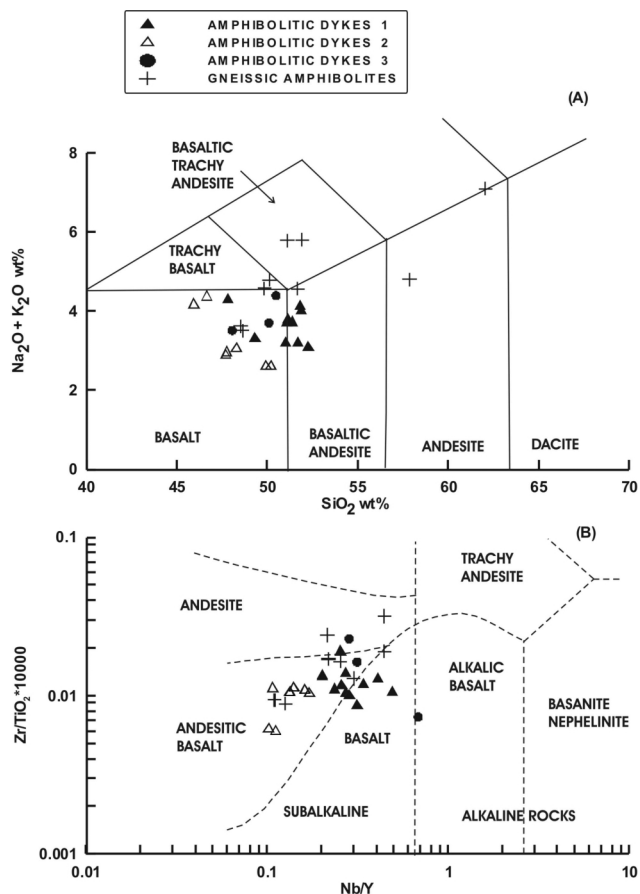


Fig. 4. (A) Plots of  $\text{SiO}_2$  vs. Total Alkali (TAS diagram: Le Bas *et al.*, 1986; Le Maitre, 1989) and (B) Nb/Y vs.  $\text{Zr}/\text{TiO}_2 \times 10000$  diagram (Winchester and Floyd, 1978) for the amphibolitic dykes 1, 2, 3 and gneissic amphibolites from Jharkhand around Dhanbad. The Nb/Y ratio acts as an alkalinity index and the  $\text{Zr}/\text{TiO}_2$  ratio acts as a differentiation index.

#### Magma type and geochemical characteristics of the dykes

In major element classification based on  $\text{Na}_2\text{O} + \text{K}_2\text{O}$  wt% versus  $\text{SiO}_2$  wt% plot (TAS diagram: Le Bas *et al.*, 1986) all of amphibolitic dykes fall within category of sub-alkaline basalt and basaltic andesite, whereas gneissic amphibolites vary in composition from basalt through basaltic andesite to andesite, straddling the alkaline-sub-alkaline divide (Fig. 4A). This, to some extent, may be due to the mobile nature of  $\text{Na}_2\text{O}$  in the gneissic amphibolites as observed in Fig. 3.1F. Based on plots of Nb/Y versus  $\text{Zr}/\text{TiO}_2 \times 10000$  (Fig. 3B: Winchester and Floyd, 1977) these rocks clearly classify as members of sub-alkaline series, ranging from basalt through andesitic basalt to andesite. Thus, above observation suggest that the alkali elements (particularly Na) may be treated with caution at least in the case of gneissic amphibolites.

Chondrite normalized rare earth elements (REE) and

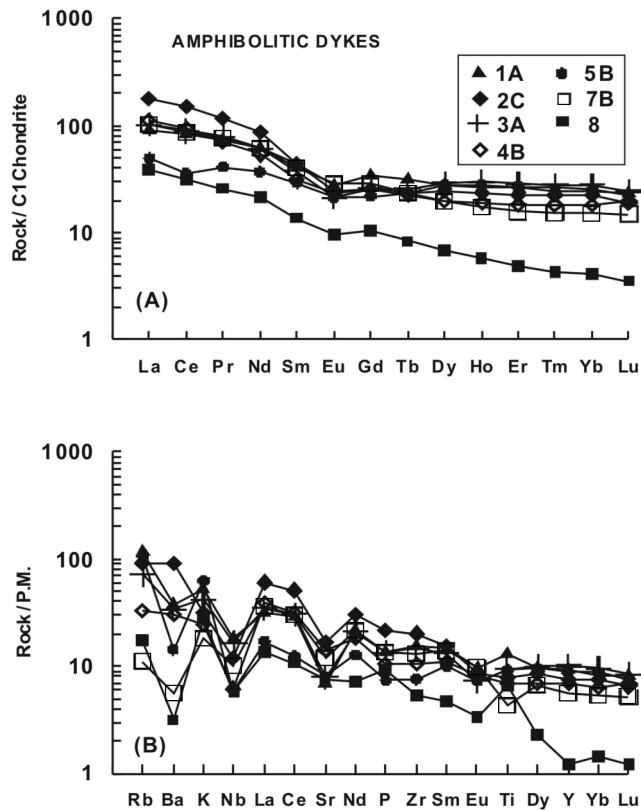


Fig. 5. (A) C1 normalized rare earth element plots and (B) Primitive mantle (P.M.) normalized multi-element patterns for representative amphibolitic dykes from Jharkhand around Dhanbad. Based on LREE-HREE ratios sample Nos. 1A, 2C, 3A belongs to Group 1, 4A, 5B represent Group 2. And 7B, 8 represent Group 3. Normalizing values after Sun and McDonough (1989).

primitive mantle normalized incompatible multi-element patterns are shown in Figs. 5 and 6. Figures 5A and B represent the REE and multi-elements patterns respectively for the amphibolitic dykes. These diagrams show the enriched patterns for incompatible trace elements especially for the light rare earth elements (LREE) and large ion lithophile elements (LILE). The amphibolitic dykes can be sub-divided into two groups (amphibolite Group 1 and Group 2) based on the LREE/HREE ratios, but within Group 1 the samples can be further subdivided into two (Group 1 and 3) based on Zr data (Fig. 3). It is interesting to note that Group 3 and 2 have similar Zr abundances but different REE patterns, for example sample Nos. 7A, 7B and 8 belonging to Group 3 has higher Gd/Yb ratios with respect to other amphibolites. Thus based on REE and Zr data the samples may be sub-divided into three sub-groups. The La/Yb ratios respectively for Group 1, 2, and 3 are: 6.995, 6.279 and 11.375 and the Zr abundance ranges from 161–264 in Group 1, 85–122 in Group 2 and 60–146 in Group 3 respectively. Among Group 3

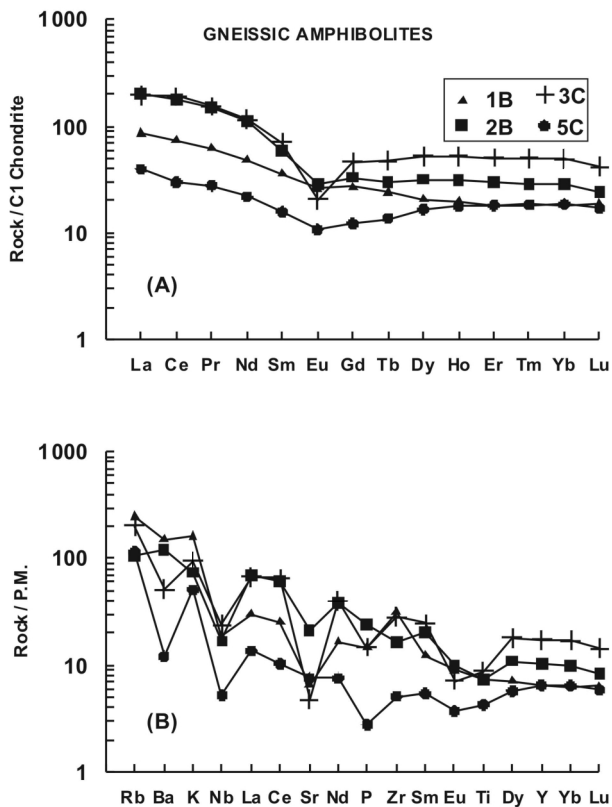


Fig. 6. (A) C1 normalized rare earth element plot and (B) Primitive mantle (P.M.) normalized multi-element patterns for representative gneissic amphibolite Jharkhand around Dhanbad. Normalizing values after Sun and McDonough (1989).

samples, number 8 has exceptionally high Gd/Yb ratios of 3.03.

Multi-element patterns in Fig. 5B depict the distinct negative anomalies for Ba, Sr and Eu. There is also depletion of high field strength elements (HFSE) especially Nb and for a few samples P and Ti (Fig. 5B). These chemical features are commonly observed in many of the continental rift volcanics (Weaver and Tarney, 1983; Thompson *et al.*, 1983; Ahmad and Tarney, 1994), present data probably indicate a similar tectonic scenario for amphibolite of the study area.

Nb/La and Nb/Ce ratios of the amphibolitic dykes range from 0.1520 to 0.878 (average  $\cong$  0.3681) and 0.07008 to 0.3857 respectively (average  $\cong$  0.1681). These values are much lower compared to Nb/La and Nb/Ce values for primitive mantle, which are 1.02 and 0.4 respectively. However, Nb/La and Nb/Ce ratios for our samples are somewhat closer to average crustal values of 0.69 and 0.33 respectively (Taylor and McLennan, 1985). Therefore, it is not possible logically to generate the observed lower ratios of Nb/La and Nb/Ce ratios of our amphibolitic dykes through crustal contamination alone.

Thus, we may have to also consider the possibility that these trace element characteristics have been obtained due to LREE-LILE enriched source characteristics with depletion of HFSE such as Nb and Ta (Weaver and Tarney, 1983; Ahmad and Tarney, 1991, 1994).

REE and multi-element spidergram patterns of gneissic amphibolites also depict enriched characteristics for LREE-LILE and depletion of HFSE (Nb, P, Ti) anomalies. The REE and multi-element patterns show large variation in their abundances with two samples having strong negative Ba, Sr and Eu anomalies (Figs. 6A and B). Observed negative anomalies for Sr and Eu in many of the studied samples may indicate fractionation of feldspar (plagioclase and K-feldspar) during evolution of the melt (Tarney and Jones, 1994). The negative Ba anomaly in some samples may be either due to alteration or involvement of K-feldspar, hornblende and/or biotite during genesis of these rocks because Ba substitutes for K in K-feldspar, hornblende and biotite.

There is considerable overlap in the REE patterns for the amphibolitic dyke and the gneissic amphibolite (Figs. 5 and 6). The La/Yb varies from 2.7 to 14.3 (average  $\cong$  7.33) and 2.6 to 6.17 (average  $\cong$  8.17) respectively for amphibolitic dykes and gneissic amphibolite. However, the REE data overall indicate that gneissic amphibolite have more fractionated patterns, as average La/Yb values for gneissic amphibolite and amphibolitic dykes are 10.52 and 8.51 respectively. LREE is also more fractionated in gneissic amphibolite as average La/Sm values for gneissic amphibolite and amphibolitic dykes are 5.1 and 4.4 respectively. However, in terms of HREE, amphibolitic dykes have more fractionated patterns than gneissic amphibolite as average Gd/Yb values for amphibolitic dykes and gneissic amphibolite are 3.87 and 1.45 respectively.

The more fractionation in HREE particularly for Group 3 of the amphibolitic dykes open the possibility is that partial melting for their source(s) might have occurred in the presence of garnet, which has significantly higher  $k_d$ 's for heavy rare earth elements (HREE) compared to the LREE (Hanson, 1980; Bender *et al.*, 1984). Thus, considering the data for the other sub-groups, at least two distinct source characteristics are indicated based on Gd/Yb ratios of the amphibolitic dyke samples. The parallel but large variation in abundances for the REE and other incompatible trace elements (Figs. 3.2, 5 and 6) probably indicate varying degree of partial melting was an important petrogenetic process, as we can not expect such large variation of highly incompatible trace elements by other processes such as fractional crystallisation alone (Hanson, 1980; Ahmad and Tarney, 1994).

The similarity of pattern for the amphibolitic dyke Group 1 and 2 and gneissic amphibolite probably suggest that they have been generated from similar sources

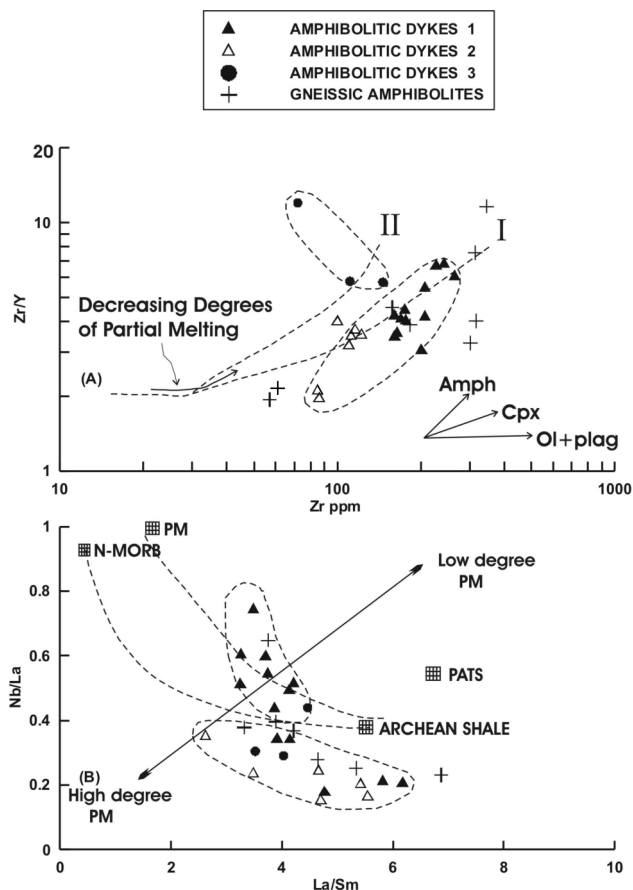


Fig. 7. (A) Binary plots of Zr vs. Zr/Y, melting curves (I and II) are after Drury (1983) and vectors for fractional crystallization are after Floyd (1993) and (B) La/Sm vs. Nb/La for the amphibolitic dykes 1, 2, 3 and gneissic amphibolites from Jharkhand around Dhanbad. Values for N-MORB, P.M. after Sun and McDonough (1989); Archean shale (AS) after Mc Lennan *et al.* (1983) and Post Archean Shale (PATS) after Taylor and Mc Lennan (1985).

or have undergone similar petrogenetic history. If they are related, they may represent different levels of emplacement of related magma and subsequent metamorphism.

#### Incompatible elements ratio-ratio plots

The ratios of incompatible trace elements such as Nb/La, La/Ce, Zr/Nb, and Zr/Sm etc. do not fractionate significantly during moderate degree of crystal fractionation of basaltic magma (Ahmad *et al.*, 1999). Whereas these ratios are sensitive to variable degrees of partial melting of mantle sources or to different kinds of sources (Weaver and Tarney, 1981; Ahmad and Tarney, 1991; Petterson and Windley, 1992). There is large variation in Zr/Y ratios with increase in Zr values (Fig. 7A). Fractionation of plagioclase and olivine cannot alter the Zr/Y ratios, but fractionation of amphibole and clinopyroxene may raise

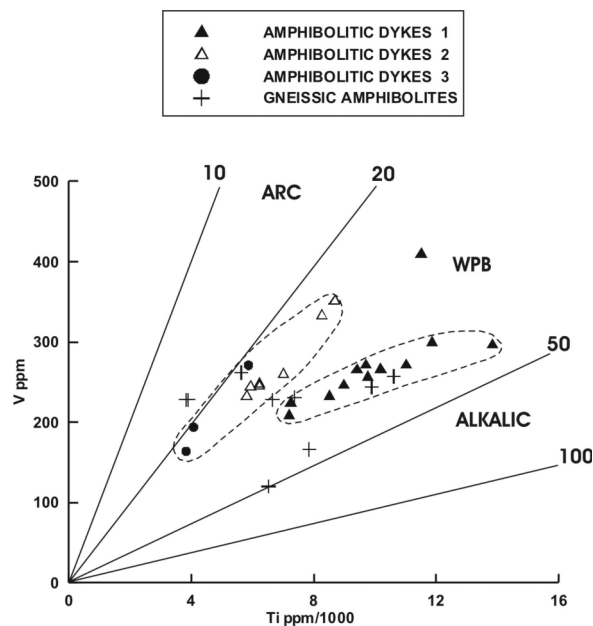


Fig. 8. Binary plot of Ti/1000 vs. V for the amphibolitic dykes 1, 2, 3 and gneissic amphibolites from Jharkhand around Dhanbad. Boundaries after Shervais (1982).

the ratio with increasing Zr content (Floyd, 1993; Ahmad *et al.*, 1999). There is large variation in Zr/Y ratios, especially for amphibolitic dykes. They can be grouped broadly in two sub-groups based on Zr/Y ratio. Such large variation of Zr/Y discounts the possibility that they were all derived by fractional crystallization of a single parental magma. Here we suggest, different parental melts, representing different degrees of partial melting of same or similar mantle source(s) is a better proposition to explain the observed data (Ahmad *et al.*, 1999). These different parental melts might have escaped the source region and fractionated independently, at various depths which may leads to the observed chemical variation in different sub-groups or they have tapped heterogeneous source(s) (Ahmad *et al.*, 1999).

In this diagram (Fig. 7A) two calculated partial melting curves (after Drury, 1983), analogous to two sets of source mineralogy (curve I: olivine 60% + opx 20% + cpx 10% + plg 10%; curve II: olivine 60% + opx 20% + cpx 10% + garnet 10%) for Archean mantle sources (Sun and Nesbitt, 1977) are also shown. Most of the samples plot between these two melting curves. There is subhorizontal shift of data points especially for the amphibolitic dykes away from the partial melting curve, this may indicate fractional crystallization of clinopyroxene  $\pm$  olivine  $\pm$  plagioclase (Floyd, 1993; Ahmad *et al.*, 1999).

It may be possible that some of amphibolitic dykes and gneissic amphibolite plotting closer to melting curve

II, were generated at greater depths in the garnet stability field. Sm/Yb ratios also suggest two different source characteristics, discussed earlier (Fig. 5A). The rest of the amphibolitic dykes appear to have been generated at intermediate depths by relatively lower but varying degrees of partial melting, followed by  $\text{cpx} \pm \text{ol} \pm \text{plg}$  fractionation.

In Fig. 7B, amphibolitic dykes and gneissic amphibolite samples clearly fall in two sub-groups. One has higher Nb/La but restricted La/Sm ratios, the other has lower Nb/La but quite variable and high La/Sm. The amphibolitic dykes and gneissic amphibolite show negative trends and have lower Nb/La but higher and variable La/Sm ratios compared to primitive mantle (PM). Such negative trend are inconsistent with partial melting of mantle source(s) alone, this is because  $D_{\text{Nb}} < D_{\text{La}} < D_{\text{Sm}}$  in mantle sources (Pearce, 1983). Thus on melting both these ratios will be highest for the lowest degree of partial melting and the ratios would decrease with increasing degrees of partial melting, giving a positive trend in this diagram (Fig. 7B). The samples appear to follow a mixing trend between N-MORB-PM and Archean shale (Fig. 7B). One of the sub-groups with higher Nb/La and restricted La/Sm nearly follow the mixing line of PM and Archean Shale. The sub-group of amphibolitic dykes with low Nb/La may not have undergone contamination by Archean shale alone because these are plotting below the mixing line between primitive mantle and Archean shale. The lower Nb/La compared to Archean shale opens the possibility for the influence of some component of Archean island arc with lower Nb/La (Martin, 1993) as a possible contaminant to explain the observed low Nb/La ratios for these samples (Fig. 7B).

#### *Tectonic setting discrimination*

Geochemistry of basaltic rocks is frequently used to discriminate tectonic settings, this is mainly because basaltic rocks are formed in almost every tectonic environment and they are believed to be geochemically sensitive to the changes in plate tectonic framework. To understand these we use multi-element and REE patterns extensively (Pearce, 1983; Holm, 1985). In addition to these, here we use Ti/1000 versus V discriminant diagram to identify palaeo-tectonic environment for these amphibolitic dykes under investigation. Ti/1000 vs. V (Shervais, 1982) plot is based on the variation in the crystal/liquid partition coefficients for vanadium, which range with increasing oxygen fugacity from  $>1$  to  $\ll 1$ . Since the partition coefficient for Ti are almost always  $\ll 1$ , the depletion of V relative to Ti is a function of the  $f\text{O}_2$  of the magma and its source, the degree of partial melting and subsequent fractional crystallization. In this diagram, the samples plot in “Within Plate Basalt” (WPB) field (Fig. 8). As discussed earlier the enrichment of LREE-LILE and depletion in

high field strength elements (HFSE: Nb, P, and Ti) also indicate rift tectonic environment (Figs. 5 and 6).

### CONCLUSION

The studied amphibolitic dykes and gneissic amphibolites are basaltic, basaltic-andesite and andesitic in composition. These dykes traverse through the Precambrian sequences of Chotanagpur gneissic complex. Most of these rocks exhibit enriched LREE-LILE and depleted HFSE characteristics, commonly observed in continental rift basalt and Proterozoic dyke swarms. They are inferred to be the product of variable degrees of partial melting of enriched mantle source(s) and subsequent fractionation of clinopyroxene  $\pm$  olivine  $\pm$  plagioclase  $\pm$  Fe–Ti oxides. They also appear to have been influenced by crustal contamination by lithologies similar to Archean shale and some components of the Archean Island Arc or their derivatives with very low Nb/La compared to the Archean shale. The Gd/Yb ratios of amphibolitic dykes indicate, at least two distinct sources, probably at two different levels with stability of garnet at the deeper source region, for the generation of mafic dykes in the study area. The enriched LREE-LILE and depletion of high-field strength elements (HFSE) especially Nb, P and Ti (Figs. 5 and 6) probably indicate generation of these dykes in a continental rift/lithospheric extension tectonic environment (Weaver and Tarney, 1983; Thompson *et al.*, 1983; Ahmad and Tarney, 1994). In addition, Ti/V diagram (Shervais, 1982) in which all the samples plot in “Within Plate Basalt” region (Fig. 8), the highly deformed (CGC) granitoid basement rocks, associated continentally derived meta-sediments and emplacement of mafic dykes all together probably indicate typical continental rift/lithospheric extension environment for generation these dykes.

**Acknowledgments**—We thank the Head of the Department of Geology, University of Delhi for providing facilities and funds for the fieldwork under the SAP provision. We thank the Director, WIHG, Dehradun for permission to analyse these samples. We especially thank Drs. M. S. Rathi, P. P. Khanna, N. K. Saini, H. K. Sachan, Chandrashekhar and all colleagues at Geochemistry Laboratory, WIHG Dehradun. We thank Dr. H. Kagi for efficient editorial handling and the two anonymous referees for their constructive comments.

### REFERENCES

- Acharyya, S. K. (2001) Geodynamic setting of the Central Indian Tectonic Zone in Central, Eastern and Northeastern India. *Geol. Surv. Ind. Spl. Pub.* **64**, 17–35.
- Ahmad, T. and Tarney, J. (1991) Geochemistry and petrogenesis of Garhwal volcanics: implications for evolution of the north Indian lithosphere. *Precambrian Res.* **50**, 69–88.

- Ahmad, T. and Tarney, J. (1994) Geochemistry and petrogenesis of late Archean Aravalli volcanics, basement enclaves and granitoids, Rajasthan. *Precambrian Res.* **65**, 1–23.
- Ahmad, T., Mukherjee, P. K. and Trivedi, J. R. (1999) Geochemistry of Precambrian mafic magmatic rocks of the western Himalaya, India: Petrogenetic and tectonic implications. *Chem. Geol.* **160**, 103–119.
- Ahmad, T., Harris, N. B. W., Islam, R., Khanna, P. P., Sachan, H. K. and Mukherjee, B. K. (2005) Contrasting mafic magmatism in the Shyok and Indus Suture Zones: Geochemical constraints. *Him. Geol.* **26**, 33–40.
- Banerji, A. K. (1991) Presidential address. Geology of the Chotanagpur region, India. *Jour. Geol.* **63**(4), 275–282.
- Bender, J. F., Hanson, G. N. and Bence, A. E. (1984) Cortland complex: differentiation and contamination in plutons of alkali basalt affinity. *Am. Jour. Sci.* **284**, 1–57.
- Bhattacharya, B. P. (1975) Structural evolution in central part of Santhal Parganas district, Bihar. *Bull. Geol. Min. Met. Soc. Ind.* **48**, 40–47.
- Bhattacharya, B. P. (1976) Metamorphism of the Precambrian rocks of the central part of Santhal Parganas district, Bihar. *Quat. Jour. Geol. Min. Met. Soc. Ind.* **48**(4), 183–196.
- Bose, M. K. (1990) Growth of Precambrian continental crust—A study of the Singhbhum segment in the Eastern Indian Shield. *Precambrian Continental Crust and Its Economic Resources* (Naqvi, S. M., ed.), *Dev. Precambrian Geol.* **8**, 267–286, Elsevier, Amsterdam.
- Bose, M. K. (1997) *Igneous Petrology*. The World Press Private Ltd, Calcutta, India.
- Chatterjee, S. R. and Sengupta, D. K. (1980) Structural and petrological evolution of the rocks around Jamua-Kakwara-Bhitia of Satpura orogeny, Bhagalpur district, Bihar. *Jour. Geol. Soc. Ind.* **21**, 171–183.
- Chattopadhyay, B. and Saha, A. K. (1974) The Neropahar pluton in eastern India: A mode of Precambrian diapiric intrusion. *Neus Jb. Miner. Abh.* **121**, 103–126.
- Clarke, G. T. (1869) Remarks upon the Basalt Dykes of the Mainland of India Opposite the Islands of Bombay and Salsette. *Quat. Jour. Geol. Soc. Lond.* **25**, 163.
- Divakara Rao, V., Subba Rao, M. V. and Ashalatha, B. (1984) Major Igneous Episodes of the Indian Sub-Continent: Geochemistry and Significance. *Geophysical Res. Bull.* **22**, 89–104.
- Drury, S. A. (1983) The petrogenesis and tectonic setting of Archean metavolcanics from Karnataka state, South India. *Geochim. Cosmochim. Acta* **47**, 317–329.
- Floyd, P. A. (1993) Geochemical discrimination and petrogenesis of alkalic basalt sequences in part of the Ankara mélange, central Turkey. *Jour. Geol. Soc. Lond.* **150**, 541–550.
- Floyd, P. A. and Lees, G. J. (1973) Ti-Zr Characterization of some Cornish pillow lavas. *Proc. Ussher Soc.* **2**, 489–494.
- Ghosh, N. C. (1971) Chemical composition of Biotite in the metamorphic and granitic rocks of Richughuta, Dist. Palamau, Bihar. *Chem. Geol.* **7**, 107–121.
- Ghosh, N. C. (1983) Geology, tectonics and evolution of the Chotanagpur granite-gneiss complex, eastern India. *Structure and Tectonics of Precambrian Rocks of India* (Sinha-Roy, S., ed.), *Recent Res. Geol.* **10**, 211–247, Hindustan Publishing Company, India.
- Ghosh, N. C., Shmakin, B. M. and Smirnov, V. N. (1973) Some geochronological observations on the Precambrians of Chotanagpur, Bihar, India. *Geol. Mag.* **110**, 481–484.
- Ghosh, N. C., Mukherjee, D. and Chatterjee, N. (2005) Plume generated Mesoproterozoic mafic-ultramafic magmatism in the Chotanagpur mobile belt of Eastern Indian Shield Margin. *Jour. Geol. Soc. Ind.* **66**, 725–740.
- Gupta, V. J. (1973) *Indian Precambrian Stratigraphy*. Hindustan Publishing Corporation, Delhi, India, 330 pp.
- Hanson, G. N. (1980) Rare earth elements in petrogenetic studies of igneous systems. *Ann. Rev. Earth Planet. Sci.* **8**, 371–406.
- Holm, P. E. (1985) The geological fingerprints of different tectonomagmatic environments using hygromagmatophile element abundances of tholeiitic basalts and basaltic andesites. *Chem. Geol.* **51**, 303–323.
- Holmes, A. (1955) Dating of Precambrian of Peninsular India and Ceylon. *Proc. Geol. Assoc. Can.* **7**, 81–106.
- Kumar, A., Dayal, A. M. and Padmakumari, V. M. (2003) Kimberlite from Rajmahal magmatic province: Sr-Nd-Pb isotopic evidence for Kerguelen plume derived magmas. *Geophys. Res. Lett.* **30**, 1–4.
- Le Bas, M. J., Le maitre, R. W., Streckeisen, A. and Zanettin, B. (1986) A Chemical classification of volcanic rocks based on the total alkali-silica diagram. *J. Petrol.* **27**, 745–750.
- Macdonald, R., Millward, D., Beddoe-Stephens, B. and Laybourn-Parry, J. (1988) The role of tholeiitic magmatism in English lake district: Evidence from dyke in Eskdace. *Min. Mag.* **52**, 459–472.
- Mahadevan, T. M. (2002) *Geology of Bihar and Jharkhand*. Geol. Soc. Ind., India, 563 pp.
- Martin, H. (1993) The mechanisms of petrogenesis of the Archean continental crust—Comparison with modern processes. *Lithos.* **30**, 373–388.
- Mazumdar, S. K. (1988) Crustal evolution of the Chotanagpur gneissic complex and the mica belt of Bihar. *Precambrian of the Eastern Indian Shield* (Mukhopadhyay, D., ed.), *Mem. Geol. Soc. India* **8**, 49–84.
- Murthy, N. G. K. (1987) Mafic dyke swarms of the Indian Shield. *Mafic Dyke Swarms* (Halls, H. C. and Fahrig, W. F., eds.), *Geol. Assoc. Canada Spl. Paper* **34**, 393–400.
- Pandey, B. K., Gupta, J. N. and Lall, Y. (1986) Whole rock and mineral Rb-Sr isochron ages for the granites from Bihar mica belt of Hazaribagh, Bihar, India. *Ind. Jour. Earth Sci.* **12**, 157–162.
- Pascoe, E. H. (1950) *A Manual of the Geology of India and Burma*. Geol. Soc. Ind. 1.
- Pearce, J. A. (1983) Role of the sub-continental lithosphere in magma genesis at active continental margins. *Continental Basalt and Mental Xenoliths* (Hawkesworth, C. J. and Norry, M. J., eds.), 230–249, Shiva Publications, Nantwich.
- Petterson, M. G. and Windley, B. F. (1992) Field relations, Geochemistry and petrogenesis of the Cretaceous basaltic Jutal dykes, Kohistan, northern Pakistan. *Jour. Geol. Soc. Lond.* **149**, 107–114.
- Pollard, P. J., Millburn, D., Taylor, R. G. and Cuff, C. (1983) Mineralogical and textural modification in granites associated with tin mineralization, Herberton, Mt Garnet Tin field,

- Queensland. *Permian Geology of Brisbane, Queensland*, Geol. Soc. Aus., Queens. Div. 413–430.
- Rao, D. R. and Rai, H. (2006) Signatures of rift environment in the production of garnet-amphibolites and eclogites from Tso-Morari region, Ladakh, India: A geochemical study. *Gond. Res.* **9**, 512–523.
- Rock, N. M. S., Griffin, B. J., Edgar, A. D., Paul, D. K. and Hergt, J. M. (1992) A spectrum of potentially diamondiferous lamproites and minettes from the Jharia coalfield, eastern India. *Jour. Volcan. Geotherm. Res.* **50**, 55–83.
- Saha, A. K. (1994) Crustal evolution of Singhbhum-North Orissa, Eastern India. *Mem. Geol. Soc. India* **27**, 341.
- Saini, N. K., Mukherjee, P. K., Rathi, M. S., Khanna, P. P. and Purohit, K. K. (1998) A new geochemical reference sample of granite (DG-H) from Dalhousie, Himachal Himalaya. *Jour. Geol. Soc. Ind.* **52**, 603–606.
- Sarkar, A. N. (1977) Structure and metamorphism of the Baraganda-Dondla area, Hazaribagh district, Bihar and their bearing on the base metal mineralisation. *Rec. Geol. Surv. Ind.* **109**(2), 170–202.
- Sarkar, A. N. (1988) Tectonic evolution of the Chotanagpur Plateau and the Gondwana basins in Eastern India: A Interpretation based on Suprasubduction Geological Processes. *Precambrian of the Eastern Indian Shield* (Mukhopadhyay, D., ed.), *Mem. Geol. Soc. Ind.* **8**, 127–146.
- Sarkar, S. N. (1968) *Precambrian Stratigraphy and Geochronology of Peninsular India*, 33. Dhanbad Publishers, Dhanbad, India.
- Sengupta, D. K. and Sarkar, S. N. (1964) Structure of the granitic rocks and associated metamorphites of the area around Muri-Silli-Jhalida, Ranchi and Purulia districts, India. *Int. Geol. Cong. Report 22nd Session, Ind.*, 374–389.
- Shervais, J. W. (1982) Ti-V Plots and Petrogenesis of modern and ophiolitic lavas. *Earth Planet. Sci. Lett.* **59**, 108–118.
- Singh, S. P. (1998) Precambrian stratigraphy of Bihar—an overview. *Ind. Precam* (Paliwal, P. S., ed.), 376–408, Scientific Publishers, Jodhpur.
- Sun, S. S. and McDonough, W. F. (1989) Chemical and isotopic systematics of Oceanic basalts: implications for mantle compositions and processes. *Magmatism in the Ocean Basins* (Saunders, A. D. and Norry, M. J., eds.), *Geol. Soc. Lond. Spec. Publ.* **42**, 313–345.
- Sun, S. S. and Nesbitt, R. W. (1977) Chemical heterogeneity of the Archean mantle composition of the bulk earth and mantle evolution. *Earth Planet. Sci. Lett.* **35**, 429–448.
- Tarney, J. and Jones, C. E. (1994) Trace element geochemistry of orogenic igneous rocks and crustal growth models. *Jour. Geol. Soc. Lond.* **151**, 855–868.
- Taylor, R. G. and Pollard, P. J. (1988) Pervasive hydrothermal alteration in tin bearing granites and implications for the evolution of ore-bearing fluids. *Granite Related Mineral Deposits* (Taylor, R. P. and Strong, D. F., eds.), *Rec. Adv. Geol.* 86–95.
- Taylor, S. R. and Mc Lennan, S. M. (1985) *The Continental Crust: Its Composition and Evolution*. Blackwell, Oxford.
- Thompson R. N., Morrison, M. A., Dickin, A. P. and Hendry, G. L. (1983) Continental flood basalts: arachnids rule OK? *Continental Basalt and Mental Xenoliths* (Hawkesworth, C. J. and Norry, M. J., eds.), 155–185, Shiva Publ., Nantwich.
- Weaver, B. L. and Tarney, J. (1981) The Scourie dyke suite: Petrogenesis and Geochemical nature of the Proterozoic subcontinental mantle. *Contrib. Min. Petro.* **78**, 175–188.
- Weaver, B. L. and Tarney, J. (1983) Chemistry of the sub continental mantle inferences from Archean and Proterozoic dykes and continental flood basalts. *Continental Basalt and Mental Xenoliths* (Hawkesworth, C. J. and Norry, M. J., eds.), 209–229, Shiva Publ., Nantwich.
- Winchester, J. A. and Floyd, P. A. (1977) Geochemical discrimination of different magma series and their differentiation products using immobile elements. *Chem. Geol.* **20**, 325–344.